Journal of Imaging Science and Technology® 63(3): 030401-1–030401-7, 2019.
© Society for Imaging Science and Technology 2019

Singular Points Detection in Fingerprints Based on Poincare Index and Local Binary Patterns

Ching-Han Chen
Department of Computer Science and Information Engineering, National Central University, Taoyuan, Taiwan, R.O.C.
E-mail: pierre@csie.ncu.edu.tw

Ching-Yi Chen
Department of Information and Telecommunications Engineering, Ming Chuan University, Taoyuan, Taiwan, R.O.C.

Tsung-Min Hsu
Department of Computer Science and Information Engineering, National Central University, Taoyuan, Taiwan, R.O.C.

Abstract. *In this study, a singular points detection method based on low-resolution image processing technique and Poincare index algorithm was introduced. First, 2D discrete wavelet transform (DWT) was used to conduct fingerprint image operation, then a LL-band image that has 1/4 resolution of the original image was obtained to reduce the operation needed in the subsequent processing. After finishing the detection procedure of singular point, each possible singular point was taken as the center to calculate the local binary pattern (LBP) features at its peripheral as reference standard for selecting correct singular point. Through this way, fake singular point is removed. The experimental result shows that the method in this study could indeed reduce the chance to detect fake singular points due to noise effect. Meanwhile, the processing speed of the traditional Poincare index method can be speeded up.*
© 2019 Society for Imaging Science and Technology.
[DOI: 10.2352/J.ImagingSci.Technol.2019.63.3.030401]

1. INTRODUCTION

Fingerprint is the texture formed by protruded and dented skin on the finger tip of human being. Each texture is filled with sweat gland to leave trace on the object touched. Ridges are the protruded sites on the fingertip surface, and valleys are dented sites on fingertip surface. Singular points, the most important global feature, contain the significant global information which is served as not only the foundation of fingerprint pattern classification but also the reference points in some fingerprint matching algorithms [1, 2].

There already exist lots of algorithms that deal with the singular point detection in the literature, and most of them are working on orientation field images [3–7]. The Poincare index method [3] is the most famous and practical approach of singular point detection. The Poincare index detects singular point using the orientation field which is calculated for each block by summing the direction changes around the selected block. It has been used by many researchers like [8, 9], and [10]. However, the Poincare index method has the ability to detect both types of singularity and it is very sensitive to noise and the variations of the grayscale level of the input image [11].

In order to improve the issues of Poincare index algorithm for its over-sensitivity on noise and easy to detect erroneous singular point at noisy images, this paper has proposed a singular points detection method applicable to low-resolution fingerprint image. First, 2D discrete wavelet transform (DWT) has been used for fingerprint image filtering to reduce the image resolution and filter out high frequency noise in the image. After the enhancement of the fingerprint image, Poincare index algorithm was used to find out all possible singular points. These reference points were used as the center to calculate the local binary pattern (LBP) feature vector at its peripheral area to enhance the correctness of singular point comparison and to reduce the opportunity of the detection of fake singular points due to noise in the fingerprint image.

2. RELATED APPROACHES

2.1 *Image Pre-Processing*

The main job of pre-processing of fingerprint image is to make normalization, texture enhancement, and noise reduction on fingerprint image so as to reserve and highlight more important texture features in the fingerprint to facilitate subsequent analysis and processing.

2.1.1 *Normalization*

Let I denote the gray-level fingerprint image, M and Var denote the estimated mean and variance of I, respectively, and G denote the normalized gray-level fingerprint image. The normalized image is defined as in Eq. (1) [12]:

$$G(i,j) = \begin{cases} M_0 + \sqrt{\dfrac{\mathrm{Var}_0^*(I(i,j)-M)^2}{Var}}, & \text{if } I(i,j) > M \\ M_0 - \sqrt{\dfrac{\mathrm{Var}_0^*(I(i,j)-M)^2}{\mathrm{Var}}}, & \text{Otherwise} \end{cases} \tag{1}$$

where M_0 and Var_0 are the desired mean and variance values, respectively.

Received May 23, 2018; accepted for publication Oct. 10, 2018; published online Feb. 25, 2019. Associate Editor: Wen-Hsiang Hsieh.
1062-3701/2019/63(3)/030401/7/$25.00



Figure 1. 2D DWT with 1-level wavelet decomposition, (a) original image, (b) four subband images.



Figure 2. Gabor filtering: (a) the original fingerprint, (b) the fingerprint after Gabor filtering.

2.1.2 *Discrete Wavelet Transform (DWT)*

DWT, due to its basis function characteristics, has the capability to do local transform of the image. It can also highlight the image texture information. DWT can decompose the image into four subbands such as LL band, LH band, HL band, and HH band [13, 14]. The LL-band signal of 2D DWT domain can retain the main part of energy and information of the original image [14–16]. Figure 1 shows the result using DWT to perform 1-level decomposition; it can be seen that the texture of LL-band image was clearest, smoothest, and, as compared to the original image, its high frequency noise was also reduced. Meanwhile, the resolution was only 1/4 of the original fingerprint image. In this study, LL-band image obtained from 1-level decomposition was used as the basis for subsequent fingerprint image analysis so as to reduce the operation of subsequent image analysis and achieve the goal of noise filtering.

2.1.3 *Gabor Filtering*

Gabor filters have emerged as one of the most commonly used techniques in the field of fingerprint enhancement. They have both frequency-selective and orientation-selective properties and have optimal joint resolution in both spatial and frequency domains [12, 17]. The mathematical expression of 2D Gabor filter is shown as Eq. (2):

$$G(x,y,\theta,f)=\exp\left\{-\frac{1}{2}\left[\frac{x_\theta^2}{\sigma_x^2}+\frac{y_\theta^2}{\sigma_y^2}\right]\right\}\cos(2\pi f x_\theta) \quad (2)$$

$$\begin{bmatrix}x_\theta\\ y_\theta\end{bmatrix}=\begin{bmatrix}\sin\theta & \cos\theta\\ -\cos\theta & \sin\theta\end{bmatrix}\begin{bmatrix}x\\ y\end{bmatrix} \quad (3)$$

where θ is the orientation of the Gabor filter, f is the ridge frequency, σ_x and σ_y are the standard deviations of the Gaussian envelope along x and y axes, respectively.

In Eq. (2), if $\theta = 90°$, the equation can be written more simply as:

$$G(x,y,f)=\exp\left\{-\frac{1}{2}\left[\frac{x^2}{\sigma_x^2}+\frac{y^2}{\sigma_y^2}\right]\right\}\cos(2\pi f x). \quad (4)$$

Therefore, as shown in Eq. (4), Gabor filter, at orientation $\theta = 90°$, can be divided into two independent functions of low-pass function and band-pass function, which were as shown in Eq. (5):

$$G(x,y,f)=G_{BP}(x,f)G_{LP}(y)=\exp\left\{-\frac{1}{2}\left(\frac{x^2}{\sigma_x^2}\right)\right\}\times\cos(2\pi f x)\exp\left\{-\frac{1}{2}\left(\frac{y^2}{\sigma_y^2}\right)\right\} \quad (5)$$

where

$$G_{BP}(x,f)=\exp\left\{-\frac{1}{2}\left(\frac{x^2}{\sigma_x^2}\right)\right\}\cos(2\pi f x),$$
$$G_{LP}(y)=\exp\left\{-\frac{1}{2}\left(\frac{y^2}{\sigma_y^2}\right)\right\}. \quad (6)$$

The texture of fingerprint image is directional, however, the background was monotonous and not directional. When operation was conducted simultaneously on directional area and non-directional area in fingerprint image through Gabor filter, it will be found that the response obtained from directional image area will be higher than that obtained from non-directional area. Therefore, through the operation result of Gabor filtering, the jobs of image enhancement and background segmentation can be realized simultaneously. Figure 2 shows the result of fingerprint image enhancement and segmentation using Gabor filter.

2.2 *Orientation Estimation*

The orientation field of a fingerprint image represents the local orientation of the ridges in a local neighborhood. It plays a very important role in fingerprint image analysis. A fingerprint image is typically divided into a number of non-overlapping blocks and an orientation representative of the ridges in the block is assigned to the block based on grayscale gradients in the block. The block orientation can be determined from the pixel gradients by averaging or voting. The orientation field of block is given by [18]:

1. Use simple gradient operators such as the Sobel operator to compute the gradients $G_x(i,j)$ and $G_y(i,j)$ at each pixel (i,j) of the input fingerprint image I:

$$G_x(i,j) = I(i,j) * S_x \begin{bmatrix} 1 & 2 & 1 \\ 0 & 0 & 0 \\ -1 & -2 & -1 \end{bmatrix} \tag{7}$$

$$G_y(i,j) = I(i,j) * S_y \begin{bmatrix} 1 & 0 & -1 \\ 2 & 0 & -2 \\ 1 & 0 & -1 \end{bmatrix} \tag{8}$$

2. Estimate the local orientation in $w \times w$ blocks:

$$V_x(i,j) = \sum_{u=i-\frac{w}{2}}^{i+\frac{w}{2}} \sum_{v=j-\frac{w}{2}}^{j+\frac{w}{2}} 2G_x(u,v)\, G_y(u,v) \tag{9}$$

$$V_y(i,j) = \sum_{u=i-\frac{w}{2}}^{i+\frac{w}{2}} \sum_{v=j-\frac{w}{2}}^{j+\frac{w}{2}} \left(G_x^2(u,v) - G_y^2(u,v)\right) \tag{10}$$

$$\theta(i,j) = \frac{1}{2}\tan^{-1}\left(\frac{V_x(i,j)}{V_y(i,j)}\right) \tag{11}$$

3. The orientation field is usually noisy, and in order to make singular points detection easier, we can use low-pass filter to adjust the erroneous local ridge orientation. However, to perform the low-pass filtering, the orientation image needs to be converted into a continuous vector field as follows [19]:

$$\emptyset_x(i,j) = \cos\left(2\theta(i,j)\right), \tag{12}$$

$$\emptyset_y(i,j) = \sin\left(2\theta(i,j)\right) \tag{13}$$

where $\emptyset_x$ and $\emptyset_y$ are the x and y components of the orientation field, respectively. The Gaussian low-pass filter can be applied as follows:

$$\emptyset'_x(i,j) = \sum_{u=-\frac{w_\emptyset}{2}}^{\frac{w_\emptyset}{2}} \sum_{v=-\frac{w_\emptyset}{2}}^{\frac{w_\emptyset}{2}} F(u,v)\emptyset_x(i-uw, j-vw), \tag{14}$$

$$\emptyset'_y(i,j) = \sum_{u=-\frac{w_\emptyset}{2}}^{\frac{w_\emptyset}{2}} \sum_{v=-\frac{w_\emptyset}{2}}^{\frac{w_\emptyset}{2}} F(u,v)\emptyset_y(i-uw, j-vw) \tag{15}$$

where F is a 2D low-pass filter of size $w_\emptyset \times w_\emptyset$ for a unit integral.

4. The final smoothened orientation field O at pixel (i,j) can be computed as follows:

$$O(i,j) = \frac{1}{2}\tan^{-1}\left(\frac{\emptyset'_y(i,j)}{\emptyset'_x(i,j)}\right). \tag{16}$$

Figure 3 shows the results of orientation estimation for a test fingerprint image.



(a) (b)

Figure 3. An example of orientation estimation, (a) original image, (b) estimated orientation field.

2.3 *Poincare Index Method*

For a digital closed curve N, the Poincare index at pixel (i,j) can be computed as follows:

$$\text{Poincare}(i,j) = \frac{1}{2\pi}\sum_{k=0}^{N-1}\Delta_k(i,j) \tag{17}$$

$$\text{where } \Delta_k(i,j) = \begin{cases} \delta_k(i,j), & \text{if } |\delta_k(i,j)| < \frac{\pi}{2} \\ \delta_k(i,j)+\pi, & \text{if } \delta_k(i,j) \le -\frac{\pi}{2} \\ \pi - \delta_k(i,j), & \text{Otherwise.} \end{cases} \tag{18}$$

$$\delta_k(i,j) = \theta\left(i_{(k+1)\bmod N}, j_{(k+1)\bmod N}\right) - \theta\left(i_k - j_k\right), \tag{19}$$

where θ is the orientation field, and $i_{(k+1)}$ and $j_{(k+1)}$ denote coordinates of the kth point on the arc length parameterized closed curve N. For our method, N is selected as 8.

The Poincare index has the values 0.5, 0, −0.5, or 1. A core point and a delta point are expected to occur at the position of which Poincare index is 0.5 and −0.5, respectively:

$$\text{Poincare}(i,j) = \begin{cases} 0.5, & \text{Core point} \\ -0.5, & \text{Delta point} \\ \text{Otherwise}, & \text{Not a Singular Point.} \end{cases} \tag{20}$$

2.4 *LBP Histograms Matching*

2.4.1 *Local Binary Pattern (LBP)*

LBP is introduced as a simple yet powerful texture descriptor for microstructures of images [20]. The LBP operator labels the pixels of an image by thresholding the neighborhood of each pixel with the center value and considers the result as an 8-bit binary string. Then, the binary string is multiplied by powers of two and summed to obtain the LBP code of the center pixel.

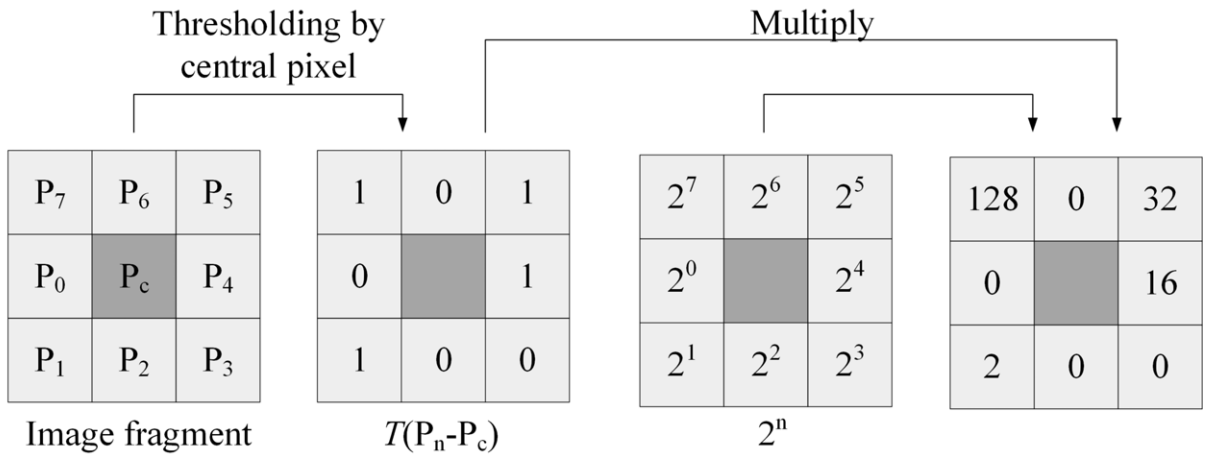


Figure 4. LBP code for 3 × 3 window.

Given a pixel, the LBP code is computed by comparing this pixel with the value of its neighbors:

$$LBP(P_c) = \sum_{n=0}^{7} T(P_n - P_c) \cdot 2^n \tag{21}$$

$$T(x) = \begin{cases} 1, & \text{if } x \geq 0 \\ 0, & \text{if } x < 0, \end{cases} \tag{22}$$

where P_c is the gray-level value of the center pixel and P_n is the gray-level value of its neighborhood. The basic form of the LBP operator is illustrated in Figure 4.

The histogram of LBP codes calculated over a region can be used as a texture descriptor. In the LBP method for texture classification, the occurrences of the LBP codes in an image are collected into a histogram. The classification is then performed by computing simple histogram similarities.

2.4.2 *Cosine Similarity*

Cosine similarity can be used to calculate the similarity between two vectors, if $x_i = (x_{i1}, x_{i2}, \ldots, x_{in})$, and $x_j = (x_{j1}, x_{j2}, \ldots, x_{jn})$, then the cosine similarity equation between x_i and x_j is:

$$\text{sim}\,(x_i, x_j) = \frac{\sum_{k=1}^{n} x_{ik} x_{jk}}{\sqrt{\sum_{k=1}^{n} x_{ik}^2} \sqrt{\sum_{k=1}^{n} x_{jk}^2}}. \tag{23}$$

3. SINGULAR POINT DETECTION SYSTEM DESIGN WITH LBP FEATURES

In this study, IDEF0 [21] in IDEF (Integrated Computer-Aided Manufacturing Definition) has been used to make hierarchical and modular design on singular point detection system. The linking relationship among all functional modules within the system was expressed by the structural analysis method. Figure 5 is our proposed IDEF0 architecture of the singular point detection system, wherein each block

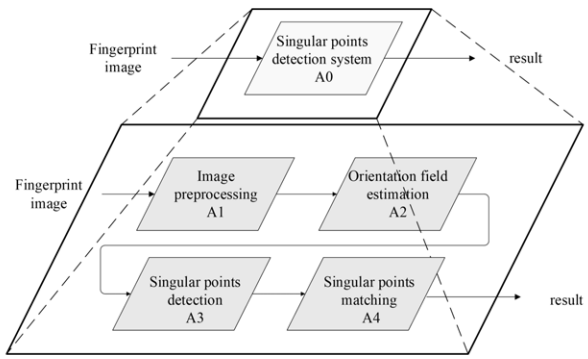


Figure 5. IDEF0 diagram of singular points detection system.

is a functional module of this system architecture, A0 is the main controller at the uppermost layer of the system, and its input is fingerprint image, and its output is the singular point match result. A0 system module can be further extended downwards as four sub-functional modules of A1–A4.

3.1 *Design of Fingerprint Singular Points Detection System*

3.1.1 *Fingerprint Image Pre-processing*

The purpose of conducting image pre-processing in this study was to reduce the resolution of fingerprint image, to filter out high frequency noise and to enhance fingerprint texture, which will speed up the processing speed of subsequent image analysis and to enhance the success rate of singular point detection. Figure 6 is the architectural diagram of the pre-processing procedure of the fingerprint image. From the figure, it can be seen that A1 was the functional module of image pre-processing, and that functional module can be further divided into several sub-functional modules such as Normalization, DWT, Gabor filtering, Otsu's binarization and Thinning.

3.1.2 *Orientation Field Estimation*

As in Figure 7, it can be seen that orientation field estimation module can be segmented into two sub-functional modules of gradient direction calculation and ridge orientation

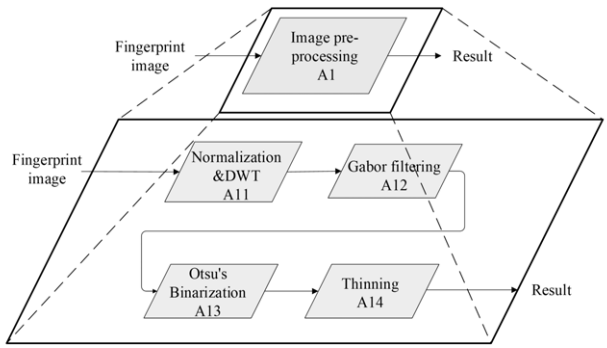


Figure 6. IDEF0 diagram of image pre-processing.

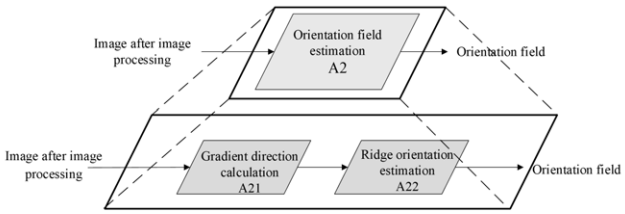


Figure 7. Orientation field estimation module.

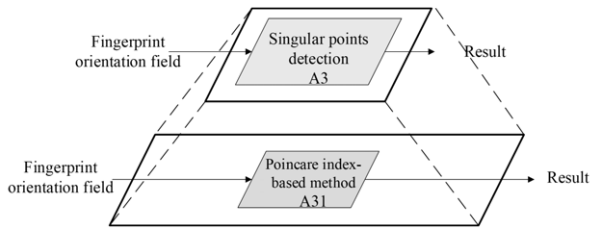


Figure 8. IDEF0 diagram of singular points detection module.

estimation. First, Eqs. (9)–(10) were used to calculate the gradient value of each pixel; subsequently, ridge orientation was estimated within each 8×8 region. Finally, through the low-pass filter, the needed smoothened orientation field was obtained.

3.1.3 *Singular Points Detection*

After finishing the orientation estimation of the fingerprint image, the Poincare index algorithm will be used to detect the location of the singular point in the fingerprint and to judge the type of singular point, wherein the IDEF0 diagram was as shown in Figure 8.

3.2 *Singular Points Matching*

In this study, the matching module of the singular point was segmented into two functional modules for design purpose, which were respectively LBP calculation module and LBP histogram matching module, as shown in Figure 9.

When Poincare index algorithm was used to detect the singular points in the fingerprint image, for many of the detected reference points, calculation will be conducted on LBP Histogram on their peripheral areas to be used as judgment basis when conducting singular point matching. First, images in the database should be calculated for their

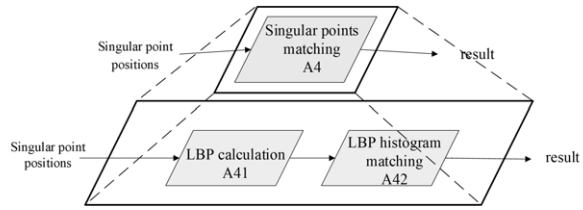


Figure 9. IDEF0 diagram of singular points matching module.

LBP features and LBP Histogram; then the LBP Histogram at the peripheral areas of singular points found for each input image was conducted for similarity matching with LBP Histogram at the peripheral areas of singular points of pre-stored image in the database. Therefore, through the texture features around the peripherals of each singular point, the correctness of singular point matching can be enhanced.

4. EXPERIMENTAL RESULTS AND DISCUSSION

4.1 *Fingerprint Image Database*

In this study, three fingerprint databases, FVC2002 [22], FVC2006 [23] and FPC, were adopted to conduct the experiment; wherein FVC2002 and FVC2006 were the open access database assigned for use by International Fingerprint Verification Competition (FVC), and both databases have very high reputation no matter in the academia or industry. Therefore, they were frequently used to test and compare the performances of many fingerprint identification algorithms and FPC was the fingerprint database constructed by us through the use of capacitive sensor. The program was tested on Intel Core i5-3230M CPU with 4GB DDRIII RAM, operating system is 64-bit windows 8.

FPC database was the fingerprint database set up by our research team through the use of the Capacitive Sensor manufactured by the company FingerPrint Cards, and it contains a total of 250 fingerprint images. The image size was 192×192, resolution was 500dpi, and sample images were as shown in Figure 10.

In our research, the block size of Poincare index algorithm is 5×5, and the digit closed curve N is selected as 8. In order to test the experimental result, two indexes such as false detection ratio (FDR) and miss detection ratio (MDR) were adopted in this study to evaluate the performances of singular point detection [24]:

$$\text{FDR}\,(\%) = \frac{\text{False Detecting Singular Points}}{\text{Total number of Singular points}} \times 100\% \tag{24}$$

$$\text{MDR}\,(\%) = \frac{\text{Missing Detecting Singular Points}}{\text{Total number of Singular points}} \times 100\%. \tag{25}$$

4.2 *Experiment Performance Evaluation*

Here the singular point detection method proposed by this study was compared with that of the traditional method, and the result was as shown in Table I. As shown in Table I, the



Figure 10. Sample images from the FPC database.

Table I. Performance comparison of the mentioned singular point detection method with that of the traditional method.

	Traditional singular point detection method			Our proposed method		
	Time cost	FDR	MDR	Time cost	FDR	MDR
FPC	210 ms	6.24%	6.58%	94 ms	5.35%	6.13%
FVC2002	827 ms	5.91%	6.32%	443 ms	6.24%	5.28%
FVC2006	750 ms	7.35%	6.75%	434 ms	6.18%	6.04%

detection rate after 1-level DWT processing was added to the singular point detection system. As compared to that of the traditional method, there will be some enhancements. Since the resolution of LL_1-band image was reduced to about 1/4 of the original fingerprint image, the average execution time was also speeded up by 48%.

For FPC database, our method has reduced two indexes of FDR and MDR by 0.89% and 0.45%, respectively. In FVC2002 database, MDR index was also reduced by 1.04%, however, FDR index increases by 0.33%; this is because in FVC2002, the contrast between background and foreground for some images was not enough. Therefore, after conducting 1-level DWT processing, the texture characteristic of the obtained LL_1-band image becomes more unclear, which was inferior to the detection of singular point. However, when this method is applied to the fingerprint image with good contrast but hazy texture, the location of the singular point can still be successfully detected. In addition, in FVC2006 database, for our method, values in two indexes such as FDR and MDR were reduced respectively by 1.17% and 0.71%, that is, it has better successful detection rate on singular point as compared to the traditional method.

5. CONCLUSION

In this study, Poincare index algorithm was adopted to conduct singular point detection on LL-band image after one-level DWT. Through DWT, more important low frequency information in the fingerprint image was preserved, and the resolution of the fingerprint image was also reduced. Therefore, the calculation cost of subsequent image analysis was greatly reduced. In addition, in singular point matching stage, through the matching of LBP Histogram at the peripheral of singular point, reference points of lower similarities were excluded, so the correctness of singular point matching can be effectively enhanced. Therefore, the method proposed by this study, as compared to the traditional method, not only has higher and correct detection rate, but also has greatly reduced average execution time. Hence, it is very suitable to be applied to the embedded application system that needs high speed execution.

REFERENCES

[1] K. C. Chan, Y. S. Moon, and P. S. Cheng, "Fast fingerprint verification using subregions of fingerprint images," IEEE Trans. Circuits Syst. Video Technol. **14**, 95–101 (2004).

[2] Z. Qinzhi and Y. Hong, "Fingerprint classification based on extraction and analysis of singularities and pseudo ridges," Pattern Recognit. **37**, 2233–2243 (2004).

[3] M. Kawagoe and A. Tojo, "Fingerprint pattern classification," Pattern Recognit. **17**, 295–303 (1984).

[4] V. S. Srinivasan and N. N. Murthy, "Detection of singular points in fingerprint images," Pattern Recognit. **25**, 139–153 (1992).

[5] K. Nilsson and J. Bigun, "Localization of corresponding points in fingerprints by complex filtering," Pattern Recognit. Lett. **24**, 2135–2144 (2003).

[6] A. K. Jain, P. Salil, L. Hong, and P. Sharath, "Filter bank-based fingerprint matching," IEEE Trans. Image Process. **9**, 846–859 (2000).

[7] L. Wang and M. Dai, "Extraction of singular points in fingerprints by the distribution of Gaussian-Hermite moment," *First Int'l. Conf. on Distributed Frameworks for Multimedia Applications* (IEEE, Piscataway, NJ, 2005), pp. 206–209.

[8] M. Liu, X. Jiang, and A. C. Kot, "Fingerprint reference-point detection," EURASIP J. Adv. Signal Process. **2005**, 498–509 (2005).

[9] C. H. Park, J. J. Lee, M. J. T. Smith, and K. H. Park, "Singular point detection by shape analysis of directional fields in fingerprints," Pattern Recognit. **39**, 839–855 (2006).

[10] M. Liu, "Fingerprint classification based on Adaboost learning from singularity features," Pattern Recognit. **43**, 1062–1070 (2010).

[11] A. I. Awad and K. Baba, "Efficient fingerprint classification using singular point," Int. J. Digit. Inf. Wirel. Commun. **1**, 611–616 (2011).

[12] L. Hong, Y. Wan, and A. K. Jain, "Fingerprint image enhancement: algorithm and performance evaluation," IEEE Trans. Pattern Anal. Mach. Intell. **20**, 777–789 (1998).

[13] W. Sweldens, "The lifting scheme: A custom-design construction of biorthogonal wavelets," Appl. Comput. Harmon. Anal. **3**, 186–200 (1996).

[14] C. H. Hsia, J. S. Chiang, and J. M. Guo, "Memory-efficient hardware architecture of 2-D dual-mode lifting-based discrete wavelet transform," IEEE Trans. Circuits Syst. Video Technol. **23**, 671–683 (2013).

[15] C. H. Hsia, "Improved finger vein pattern method using wavelet-based for real-time personal identification system," J. Imaging Sci. Technol. **62**, 30402 (2018).

[16] C. H. Hsia, "New verification method for finger-vein recognition system," IEEE Sensors J. **18**, 790–797 (2018).

[17] A. K. Jain and F. Farrokhnia, "Unsupervised texture segmentation using Gabor filters," Pattern Recognit. **24**, 1167–1186 (1991).
[18] E. Zhu, J. Yin, C. Hu, and G. Zhang, "A systematic method for fingerprint ridge orientation estimation and image segmentation," Pattern Recognit. **39**, 1452–1472 (2006).
[19] S. Gayathri and V. Sridhar, "FPGA implementation of orientation field estimation of fingerprint recognition process," Int. J. Recent Trends Eng. Technol. **11**, 132–143 (2014).
[20] T. Ojala, M. Pietikainen, and D. Harwood, "A comparative study of texture measures with classification based on feature distributions," Pattern Recognit. **29**, 51–59 (1996).
[21] R. J. Mayer, "IDEF0 function modeling". A reconstruction of the original Air Force Wright Aeronautical Laboratory Technical Report (1992).
[22] D. Maio, R. Maltoni, J. Cappelli, J. Wayman, and A. Jain, "FVC2002: Fingerprint verification competition," IEEE Trans. Pattern Anal. Mach. Intell. **24**, 402–411 (2002).
[23] R. Cappelli, M. Ferrara, A. Franco, and D. Maltoni, "Fingerprint verification competition 2006," Biom. Technol. Today **15**, 7–9 (2007).
[24] Y. Mei, R. Hou, and J. Wang, "An improved method for fingerprints' singular points detection based on orientation field partition," Int. J. Signal Process. Image Process. Pattern Recognit. **6**, 225–233 (2013).